Non-Linear Discharge of Human Motor Units During Linear Time-Varying Contractions Across Motor Pools

D. McAuliffe[1], T. Kmiec[1], C. Taylor[2], C. Thompson[1]

1. Department of Health and Rehabilitation Sciences, College of Public Health, Temple University
2. Department of Kinesiology, College of Public Health, Temple University
danielle.mcauliffe@temple.edu, tek@temple.edu, taylor.chris@temple.edu, ckt@temple.edu

Abstract: Increasing muscular force occurs when motor units, comprised of the spinal motor neuron and innervating muscle fibers, increase firing rates, or when the number of motor units recruited within that muscle increases[1][2]**. It is known that the recruitment limb of increasing linear force generation can elicit nonlinear firing rate patterns, and that the firing rate at the point of recruitment of motor units is higher than the firing rate at de-recruitment.**[3] **To the best of our knowledge, the de-recruitment limb firing rates during decreasing torque generation have yet to be characterized. We sought to test whether over the course of a linearly increasing and decreasing torque generation, we would observe similar and linear behavior of firing rates. High density surface EMG (HD-EMG) recordings of a human subject were decomposed into motor units during contractions using blind source separation. 13 subjects were analyzed over 10s triangular torque contractions. Slopes of firing rates vs time over the course of isometric triangular torque generation were generated using a bilinear fit for both the recruitment and de-recruitment limbs. Residuals of raw firing rates for the lines of best fit before and after the breakpoint were calculated. Linear increases and decreases in torque are accompanied by nonlinear increases and decreases in firing rates. These results suggest important characteristic intrinsic mechanisms to the sustained and released firing activity of motor neurons.**

I. Introduction

An increase in muscle force generated by motor units, comprised of the spinal motorneuron and the muscle fibers it innervates, results from an increase in firing rate or an increase in the number of motor units recruited within that muscle. Over the course of linearly increasing torque, motor unit firing rates are non-linear[3]. It is often the case there is a rapid increase in discharge rate at onset followed by and more linear change in discharge termed[4]. The underlying mechanisms of this non-linearity behavior are consistent with the relatively slow voltage dependent activation of persistent inward Ca2+ and Na+ currents (PICs) on the soma and proximal dendrites of the spinal motoneurons[5] [6][7].

The activation of spinal motoneurons is often thought to be due to solely the passive integration of synaptic drive from cortical or reflexive sources, however these active properties of motoneurons (e.g. PICs) have a fundamental role in the discharge of spinal motoneurons [7][8]. Further PICs can be modulated via norepinephrine, serotonin, and other monoamines from the brainstem[9][10][7][11]. These PICs can activate at sub-threshold levels, allowing for an amplified output compared to excitatory synaptic activity and persistent activity, which is highly sensitive to synaptic inhibition[12][3]. Modification of intrinsic mechanisms of motor neurons has significant impact of both typical and abnormal motor systems including within spinal cord injury, stroke, and spasticity[13][12]. It is crucial to understand how changes in motor neuron excitability adjusts firing rates and subsequent output of force generation.

The purpose of this study is to describe approaches to quantify the linearity of the motor unit discharge patterns during linear activation and deactivation of the motor pool. To assess both the activation and deactivation of the motoneuron, this approach is applied to both the linear ascending and descending limbs of the contraction to quantify the presence and magnitude of potential bilinear behavior of spinal motoneurons. Further, this approach is demonstrated in several muscles and may have utility in the assessment of neuromuscular function in neurological injury.

II. EMG Collection

Thirteen adults with no reported neuromuscular impairments participated in a single day of testing. EMG data was collected through high density surface electrode arrays. This 13 x 5 electrode montage (8 mm interelectrode distance) is affixed to the abraded and cleaned skin over the belly of the target muscle. EMG data is amplified 100x, filtered 10 – 900 Hz, and collected at 2048 Hz at 16 bit precision synchronously with the torque data (Quattrocento; OT Bioelettronica; Turin, IT). Participants were seated comfortably in with their tested extremity rigidly affixed to a six degree of freedom load cell (JR3; Woodland, CA). After assessing peak force generation from three maximum voluntary contractions (MVC), participant generated linearly increasing force to 20% of their max volitional contraction (MVC) over 10s, followed by 10s of linearly decreasing force back to rest with the assistance of a visual torque feedback overlaid upon the ramp target[14]. This protocol was performed in four different muscles chosen for being functionally distinct, superficial, and have known differences in motor

unit discharge patterns: tibialis anterior (TA; n=3), first dorsal interosseous (FDI; n=3 subjects), medial gastrocnemius (MG; n=3 subjects), and soleus (Sol; n=3).

III. Spike train analysis

HD-EMG was decomposed by a convoluted blind source separation [15]. Such an approach maximizes the sparcity of independent sources and has been well validated. A total of 124 spike trains were decomposed across all contractions. Every discharge of each spike train was manually confirmed. When missasignments were apparent, a semi-automated tool was used to remove the suspect cluster and perform a local reoptomization of the cost function used for the decomposition to more accurately identify discharges[14][15]. Motor units were included in the analysis if they had at least 15 spikes and 3 seconds of firing during ascending limb of the contraction (n=108). For each spike train, the time of each spike is plotted against the instantaneous discharge frequency and smoothed using a 1s Hanning window. The initial, maximal, and final discharge rates are calculated from the windowed discharge times. Additionally, the time of recruitment, relative to the start of the contraction was taken as a measure of recruitment order and estimate of the size of the motoneuron[6].

Clear non-linearities are observed in discharge pattern of human motor units in both the ascending and descending limbs of the linear time varying contraction.[3] To quantify the non-linearity, each motor unit spike train was divided into recruitment and de-recruitment limb at the peak of the submaximal contraction. We then applied bilinear fits using multiple approaches in an exploratory fashion where lines of best fit were visually inspected overlaying raw data points to confirm the fit that best characterized the raw data. Unconstrained and constrained approaches to maximize two linear fits are implemented using both the instantaneous discharge rates and smoothed discharge rates. Constrained refers to limiting the time at which a break point can occur to prevent skewed breaks at the extreme ends of the limb. Strengths and limitations of these methods are described in results. The separation point designated to distinguish segments was the point at which the combined r-squared values were the highest the unconstrained approach. This point will be referred to as the breakpoint and these four segments will be referred to throughout as Ascending Initial (AI) and Ascending Final (AF) for the recruitment limb and as Descending Initial (DI) and Descending Final (DF) for the de-recruitment limb. For graphical purposes the derecruitment limb is mirrored in time.

IV. Results: Bilinear fits

Figure 1 shows an example of decomposition of multiple motor unit spike trains as subject linearly increased torque generation to 20% of MVC over the course of 10s and subsequently decreased back to baseline over 10s. When the instantaneous motor unit discharge rate is plotted against time, this motor units increased firing rate

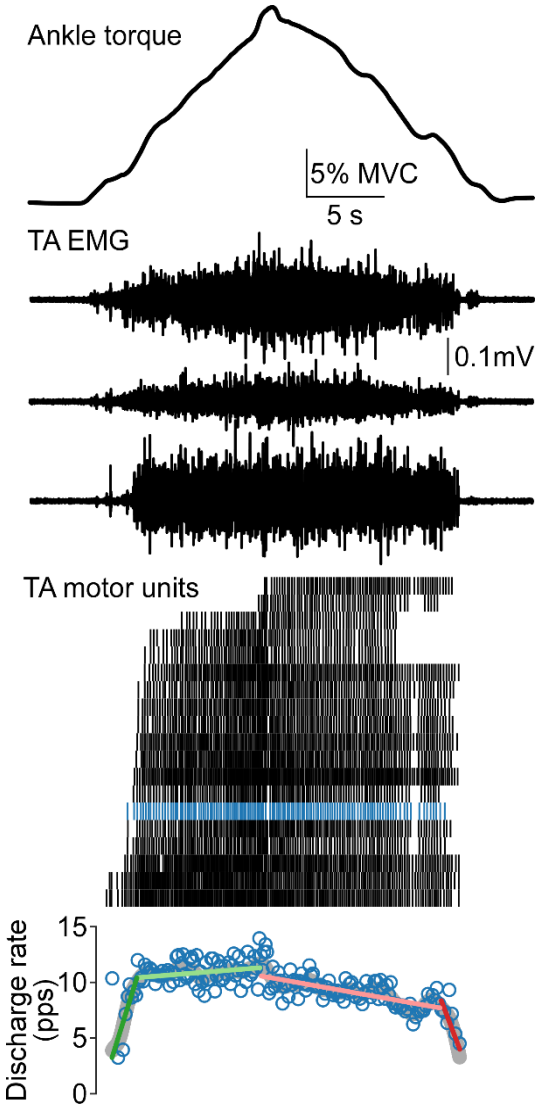

Figure 1 Decomposition of Motor Unit Motor units decomposed from TA over linearly increasing and decreasing torque. Torque trace is shown in the top panel with three representative EMG channels below. A raster of the decomposed motor unit spike trains are shown under the EMG. Bottom Panel shows a single motor unit's firing rates against time. The AI (green), AF (light green), DI (light red), DF (red) line of best fit is shown overlaying the raw firing rates, illustrating the fit to the raw data.

along this trajectory during the recruitment limb and decreased during the de-recruitment limb.

To establish the breakpoint within the recruitment and subsequent de-recruitment limbs we attempted 4 methods to generate lines of best fit that visually overlaid the raw discharge rates. The panels of **Figure 2** show these attempts as histograms of the number of spikes contained before the breakpoint in the recruitment limb (solid line) and after the breakpoint in the derecruitment limb (dashed line), The first attempted an unconstrained

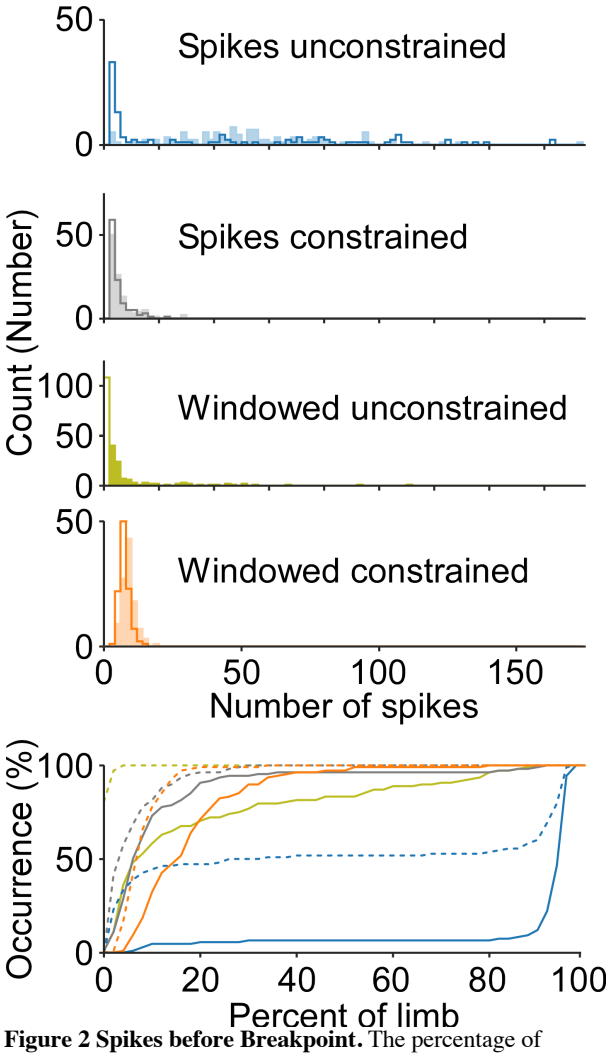

Figure 2 Spikes before Breakpoint. The percentage of motor unit break points with respect to percentage of length of motor unit firing is depicted in the bottom panel. Histograms of the size of limbs in each breakpoint analysis iteration are shown in the top 4 panels. Shaded lines in the top panels and dashed in the bottom panel depict the ascending limb breakpoint, with descending limb breakpoints being depicted buy solid lines throughout. Unconstrained motor units have the majority of breakpoints very early and very late into firing. The constrained motor units shift towards the very beginning and have breakpoints with the least amount of points available.

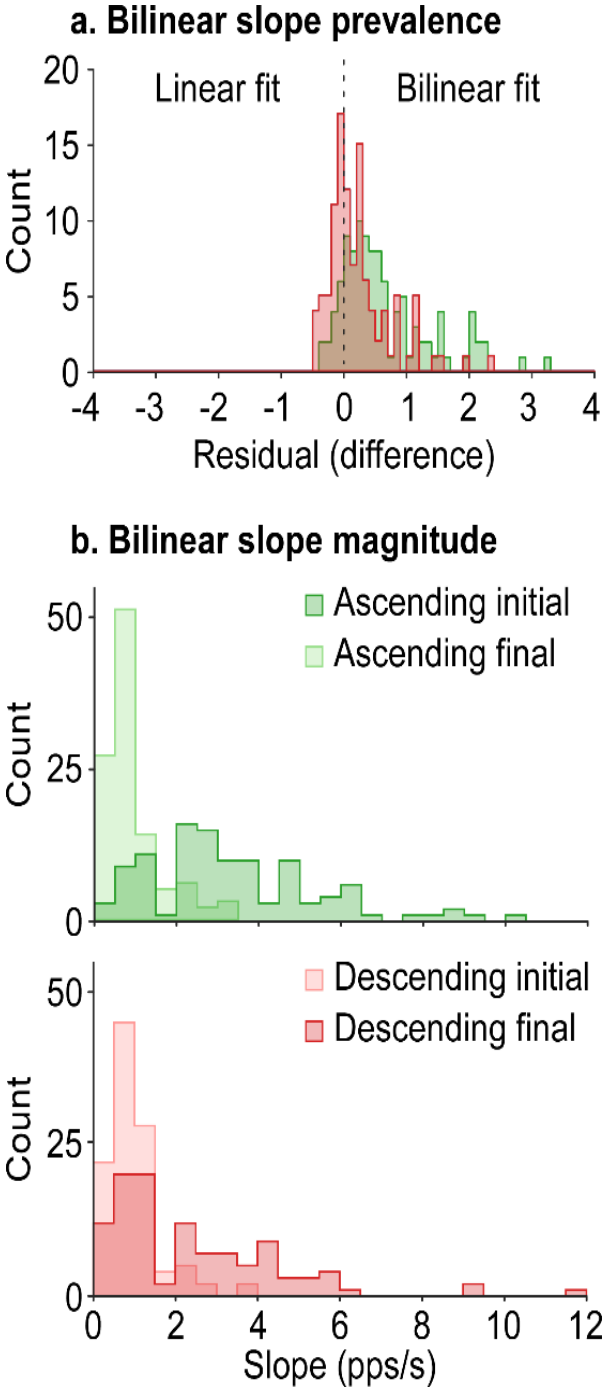

Figure 3 Bilinear slope prevalence and magnitude. a. The prevalence of improved bilinear fits over linear fits shown by the histogram of differences between residuals of generated slope and extrapolated slope. This is used to determine which slopes better characterize firing rate patterns of the separate limbs. b. The magnitude of the corrected slopes of recruitment initial(dark green) and final (light green) and derecruitment initial (dark red) and final (light red) show the distributinos of the steepness of the slopes

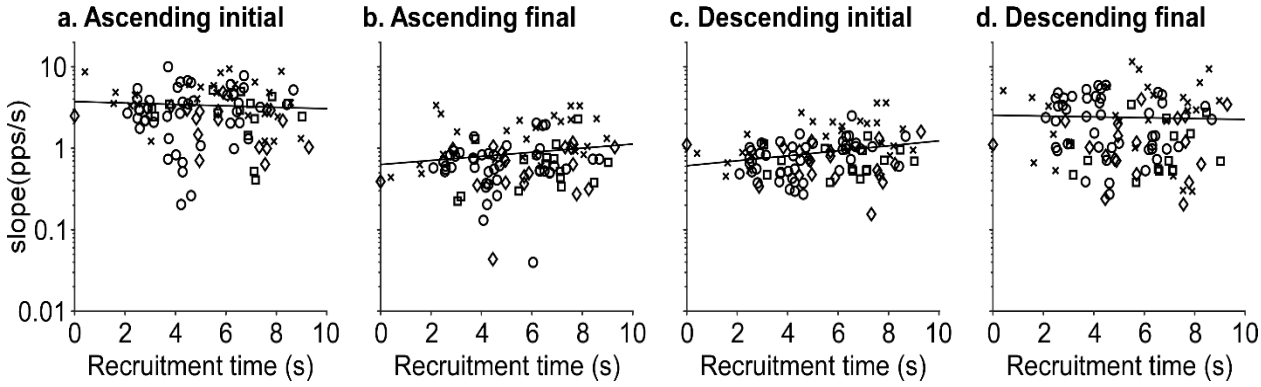

Figure 4. Correlations between slopes and recruitment. a: AI slope, no correlation. b: AF slope is significantly correlated to the time of recruitment of each motor unit (r = .19 p <0.05). c: DI slope is significantly correlated with recruitment time of each motor unit (r = 0.25 p <0.01) d: DF slopes, no correlation. ○=TA x=FDI □=Sol ◊=MG

iterative linear regression. However, using this method resulted in segments that captured the least amount of points on both the front and back ends, often with negative initial slopes, and upon visual inspection, did not fit the raw data. This is not completely unexpected, as there is significant variability in the firing rates of spike trains. Constraining the breakpoint to the within the first 2 seconds yielded only slightly better results and offer limbs skewed towards using the least amount of points at the beginning. To address this issue, a 1s hanning window was applied to the data, allowing for a line of best fit across the smoothed and interpolated signal. However, this comes at a cost. Filtering data can produce edge effects. Using an unconstrained breakpoint we observe a shift similar to the unconstrained unfiltered fits, biased towards using the least points possible. These fits can be misleading by using a breakpoint from a time point that is shorter than the filter. To mitigate the effects of the filter distortions, we forced a breakpoint at 1s into firing for each motor unit. Upon visual inspection, the addition of a filter greatly improved the fit of the slopes to the raw data and increased the number of spikes captured. The bottom panel of **Figure 2** illustrates the cumulative sum of these breakpoints in each of the 4 methods in both the ascending (solid line) and descending (dotted) and is helpful to consider due to the fact that number of spikes varies.

V. Results: Non-linear motor unit discharge during ascending and descending phases

The prevalence of nonlinearities within the recruitment and de-recruitment limbs would be confirmed by the comparison of the two slopes within each limb and the comparison of the residuals of the raw data using the extrapolated lines of best fit from all segments. If the aggregate residuals of the best fit line generated in the initial ascending and final descending segments are less than the aggregate residuals of the best fit lines generated from the middle segments, it would support the hypothesis that there is in fact a break point where the slopes of the firing rates shallow in both limbs. Recognizing that a subset of motor units are better characterized by a linear fit, differences between residuals of the extrapolated middle segment slopes and their respective initial and final slopes were calculated. Within this cohort of motor units, we observe 13% of motor units are better represented by the linear fit in the recruitment limb, and 39% within the de-recruitment limb (**Figure 3a**). AI and DF segments with an extrapolated better fit are corrected to the extrapolated slope during further analyses.

The magnitude of slopes are shown in **Figure 3b**. Both the ascending and descending phases show steep slopes at the recruitment and derecruitment of motor units. Subjects' AI slopes *(m. 3.38 std. 2.22)* were significant steeper than their AF slopes *(m. 0.93 std. 0.73 p<0.0001*). Additionally, the line of best fit for the AI segement better matched the raw data than the line of best fit of the AF segment overall, given that the differences in residuals were significantly different than 0 (**Figure 3a**) for both the recruitment and derecruitment limbs (*both p<0.0001*) The nonlinearity of the ascending limb has been well characterized and these results are in line with previous literature. However, the characterization of the descending limb remains ambiguous. The results in **Figure 3b** suggest that the DF segment slopes are significantly steeper than the DI segment slopes (*m. 2.2 std. 2.1, m. 1.0 std. 0.6 respectively, p <0.0001*). and although not identical, produces similar distributions. These comparisons indicate a significant change in the slope of firing rates during a linearly increasing torque generation, and more notably during a linearly decreasing torque generation.

VI. Results: Variations within and across motor pools

We have established that 4 distinct segments govern the firing rate of the motor unit. If we assume that these separate slopes are generated from separate mechanisms, which, if either, is dependent on the context and which segment is independent? To address this question,

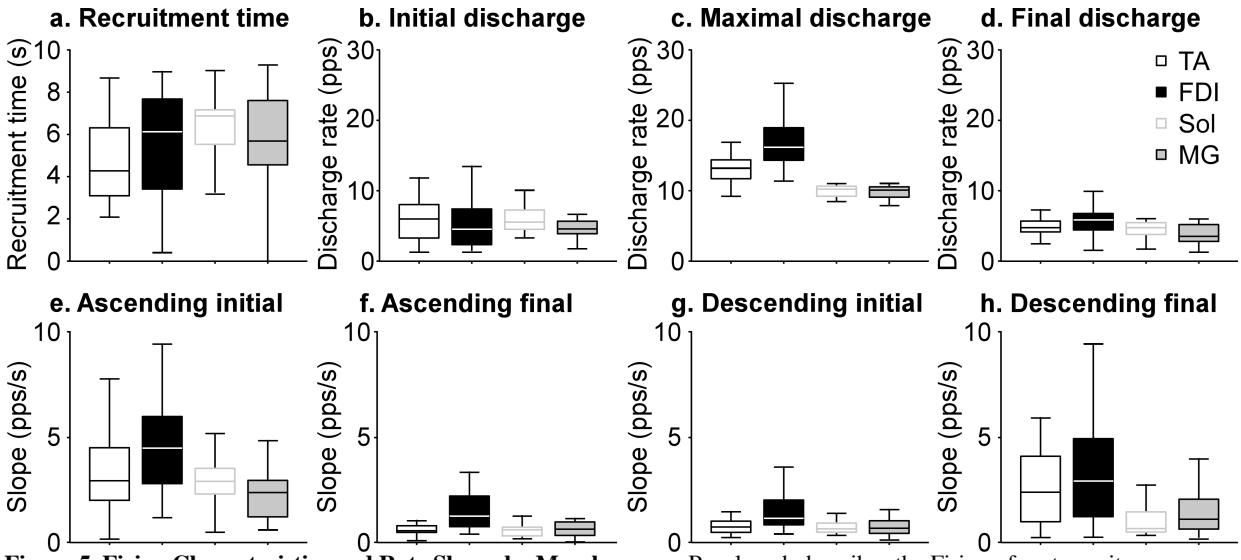

Figure 5 Firing Characteristics and Rate Slopes by Muscle group. Panels a-d. describes the Firing of motor unit (recruitment time, initial, max, and final firing rates left to right) Panels e-h. (AI, AF, DF, DI) describes the slopes of best fit within that segment of each muscle group.

correlations between slopes and recruitment time are assessed. (**Figure 4**). While no significant relation between recruitment time and AI or DF slopes exist, the AF and DI slopes both show weak linear relationships with recruitment time (*r = 0.19,2.5 respectively)*. This suggests that with an increase in recruitment time, the middle segment slopes become steeper, and that the initial and final firing rate slopes are independent of recruitment time.

Do these patterns of firing look similar between different muscle groups? At a trend level, FDI motor units have steeper slopes in all segments of firing, and a higher max firing rate (**Figure 5**). This is consistent with previous results illustrating that FDI uses a higher firing rate to achieve the same effort[16] of torque generation as the TA, LG, and Sol muscle groups.

VII. Summary

In this paper, we investigate the properties of motor unit firing rates during linear and symmetrical ramp contractions and illustrated the nonlinearity in the de-recruitment limb of firing rates. HD-EMG and subsequent motor decomposition offers advantages over traditional EMG data collection being non-invasive, yielding data from a larger amount of motor units simultaneously, providing information regarding a larger proportion of the motor pool, allowing for less training involved in data collection, and increasing comfort for subjects and patients[14][16][6][15]. These methods offer an opportunity for researchers and clinicians to provide detailed quantification of the discharge of populations of motor units.

For the recruitment limb, it is established that a singular linear fit is present in ~10% of motor units[3]. These motor units are exposed by finding the negative values of the subtraction of the residuals (**Figure 3**). When this is the case, slopes for the AI and DF segments are replaced by the slopes for their respective middle limb slopes. After replacement of slopes for these motor units to ensure true fits, to answer our hypothesis of whether or not the bilinear fit accurately captures the data of both limbs, comparisons between the AI and AF slopes to the DI and DF slopes are performed. To further characterize motor unit behavior in these limbs we observed the properties within different muscle groups with respect to recruitment time.

We characterize the bilinear fits of motor neuron activation and inactivation. Consistent with previous work, ascending limbs in 89% of motor units increasing the understanding of mechanisms units demonstrate a bilinear fit[3]. This is likely due to the activation of the PIC contributing to the initial onset of discharge[17]. Further, we are able to quantify the offset bilinear fit – this occurs less often, though still occurs in nearly two third of motor units. This may be due to the deactivation of the PIC. Such deactivation of the PIC during repetitive discharge has been observed in computer simulations [18], but has not been described in human discharge patterns. Further, these bilinear fits demonstrate an AI and corresponding DF segment that are consistently 2-4x steeper than the AF and DI segments.

These steeper initial and final slopes are not correlated with recruitment time (**Figure 4a,d.**), whereas the middle portions are correlated with recruitment order with later recruitment units correlating with a steeper slope (**Figure**

4b,c). While this seems paradoxical to the onion skin theory of motor unit activation[19], with later recruited motor units exhibiting lower firing rates [2], these larger, later recruited, motoneurons will have a shorter afterhyperpolarization allowing for a greater increase in discharge rates[20]. We observe these segments generally across muscle groups, however more research is needed to determine whether and how these fits might differ. We see that these slopes steepen in FDI and have a higher max firing rate. Differences in firing rate behavior of diverse muscles could shed light on both normal and clinical physiology.

Understanding the nonlinear characteristics of the motor unit firing rates is important when assessing both the synaptic drive and excitability of motoneurons, which together contribute to the discharge of motor units[13][21]. The effect of PICs on motoneuron firing patterns has important implications for both the weakness and spasticity observed following upper motor neuron lesions[22][23]. These results support the notion that sustained activation of the PIC decrease the amount of synaptic drive needed to maintain the same force output in recruitment and de-recruitment limbs [13] and that the PIC vulnerability to inhibition during the de-recruitment limb could contribute to the non-identical firing rate slopes. We suggest that differing physiological mechanisms govern the separate segments within the recruitment and de-recruitment limbs to allow for the changes in slopes and that those may not echo one another. The initiation of PICs allows for the AF segment to shallow as input increases, but the inhibitory mechanisms are more jarring to the system, giving steeper DI firing rates, and also necessitate for less excitatory input to maintain the respective force generation as in the recruitment limb. Future research should take these nonlinear characteristics into account when investigating motor units, and future directions can include observing asymmetry of these relationships and how motor unit behaviors change over multiple contractions.

ACKNOWLEDGMENTS

Research reported in this publication is supported by the NIH (NS098509 to CKT)

References

[1] E. D. Adrian and D. W. Bronk, “The discharge of impulses in motor nerve fibres: Part II. The frequency of discharge in reflex and voluntary contractions,” *J. Physiol.*, vol. 67, no. 2, pp. i3-151, Mar. 1929.

[2] C. J. De Luca and E. C. Hostage, “Relationship Between Firing Rate and Recruitment Threshold of Motoneurons in Voluntary Isometric Contractions,” *J. Neurophysiol.*, vol. 104, no. 2, pp. 1034–1046, Aug. 2010, doi: 10.1152/jn.01018.2009.

[3] A. J. Fuglevand, R. A. Lester, and R. K. Johns, “Distinguishing intrinsic from extrinsic factors underlying firing rate saturation in human motor units,” *J. Neurophysiol.*, vol. 113, no. 5, pp. 1310–1322, Mar. 2015, doi: 10.1152/jn.00777.2014.

[4] C. J. de Luca, R. S. LeFever, M. P. McCue, and A. P. Xenakis, “Behaviour of human motor units in different muscles during linearly varying contractions,” *J. Physiol.*, vol. 329, pp. 113–128, 1982.

[5] M. D. Binder, R. K. Powers, and C. J. Heckman, “Nonlinear Input-Output Functions of Motoneurons,” *Physiology*, vol. 35, no. 1, pp. 31–39, Dec. 2019, doi: 10.1152/physiol.00026.2019.

[6] C. J. Heckman and R. M. Enoka, “Motor Unit,” in *Comprehensive Physiology*, American Cancer Society, 2012, pp. 2629–2682.

[7] C. J. Heckman, C. Mottram, K. Quinlan, R. Theiss, and J. Schuster, “Motoneuron excitability: the importance of neuromodulatory inputs,” *Clin. Neurophysiol. Off. J. Int. Fed. Clin. Neurophysiol.*, vol. 120, no. 12, pp. 2040–2054, Dec. 2009, doi: 10.1016/j.clinph.2009.08.009.

[8] C. J. Heckmann, M. A. Gorassini, and D. J. Bennett, “Persistent inward currents in motoneuron dendrites: implications for motor output,” *Muscle Nerve*, vol. 31, no. 2, pp. 135–156, Feb. 2005, doi: 10.1002/mus.20261.

[9] C. K. Thompson, M. D. Johnson, F. Negro, L. M. Mcpherson, D. Farina, and C. J. Heckman, “Exogenous neuromodulation of spinal neurons induces beta-band coherence during self-sustained discharge of hindlimb motor unit populations,” *J. Appl. Physiol.*, p. japplphysiol.00110.2019, Jul. 2019, doi: 10.1152/japplphysiol.00110.2019.

[10] P. J. Harvey, X. Li, Y. Li, and D. J. Bennett, “5-HT2 receptor activation facilitates a persistent sodium current and repetitive firing in spinal motoneurons of rats with and without chronic spinal cord injury,” *J. Neurophysiol.*, vol. 96, no. 3, pp. 1158–1170, Sep. 2006, doi: 10.1152/jn.01088.2005.

[11] B. Fedirchuk and Y. Dai, “Monoamines increase the excitability of spinal neurones in the neonatal rat by hyperpolarizing the threshold for action potential production,” *J. Physiol.*, vol. 557, no. Pt 2, pp. 355–361, Jun. 2004, doi: 10.1113/jphysiol.2004.064022.

[12] M. D. Johnson, C. K. Thompson, V. M. Tysseling, R. K. Powers, and C. J. Heckman, “The potential for understanding the synaptic organization of human motor commands via the firing patterns of motoneurons,” *J. Neurophysiol.*,

vol. 118, no. 1, pp. 520–531, Jul. 2017, doi: 10.1152/jn.00018.2017.

[13] M. Gorassini, J. F. Yang, M. Siu, and D. J. Bennett, "Intrinsic Activation of Human Motoneurons: Reduction of Motor Unit Recruitment Thresholds by Repeated Contractions," *J. Neurophysiol.*, vol. 87, no. 4, pp. 1859–1866, Apr. 2002, doi: 10.1152/jn.00025.2001.

[14] C. K. Thompson *et al.*, "Robust and accurate decoding of motoneuron behaviour and prediction of the resulting force output," *J. Physiol.*, vol. 596, no. 14, pp. 2643–2659, Jul. 2018, doi: 10.1113/JP276153.

[15] F. Negro, S. Muceli, A. M. Castronovo, A. Holobar, and D. Farina, "Multi-channel intramuscular and surface EMG decomposition by convolutive blind source separation," *J. Neural Eng.*, vol. 13, no. 2, p. 026027, Feb. 2016, doi: 10.1088/1741-2560/13/2/026027.

[16] C. Taylor, T. Kmiec, and C. Thompson, "Differences in Human Motoneuron Excitability Between Functionally Diverse Muscles," *CommonHealth*, vol. 1, no. 1, Art. no. 1, Apr. 2020, doi: 10.15367/ch.v1i1.300.

[17] H. S. Milner-Brown, R. B. Stein, and R. Yemm, "Changes in firing rate of human motor units during linearly changing voluntary contractions," *J. Physiol.*, vol. 230, no. 2, pp. 371–390, Apr. 1973.

[18] R. K. Powers and C. J. Heckman, "Synaptic control of the shape of the motoneuron pool input-output function," *J. Neurophysiol.*, vol. 117, no. 3, pp. 1171–1184, Mar. 2017, doi: 10.1152/jn.00850.2016.

[19] C. J. De Luca and Z. Erim, "Common drive in motor units of a synergistic muscle pair," *J. Neurophysiol.*, vol. 87, no. 4, pp. 2200–2204, Apr. 2002, doi: 10.1152/jn.00793.2001.

[20] C. J. De Luca and P. Contessa, "Biomechanical benefits of the Onion-Skin motor unit control scheme," *J. Biomech.*, vol. 48, no. 2, pp. 195–203, Jan. 2015, doi: 10.1016/j.jbiomech.2014.12.003.

[21] M. Gorassini, J. F. Yang, M. Siu, and D. J. Bennett, "Intrinsic Activation of Human Motoneurons: Possible Contribution to Motor Unit Excitation," *J. Neurophysiol.*, vol. 87, no. 4, pp. 1850–1858, Apr. 2002, doi: 10.1152/jn.00024.2001.

[22] A. Méndez-Fernández, M. Moreno-Castillo, N. Huidobro, A. Flores, and E. Manjarrez, "Afterdischarges of Spinal Interneurons Following a Brief High-Frequency Stimulation of Ia Afferents in the Cat," *Front. Integr. Neurosci.*, vol. 13, Jan. 2020, doi: 10.3389/fnint.2019.00075.

[23] B. A. Conway, H. Hultborn, O. Kiehn, and I. Mintz, "Plateau potentials in alpha-motoneurones induced by intravenous injection of L-dopa and clonidine in the spinal cat.," *J. Physiol.*, vol. 405, pp. 369–384, Nov. 1988.